



PAPER

Thermal conductivity, diffusivity and specific heat capacity of as-grown, degenerate single-crystalline ZnGa₂O₄

OPEN ACCESS

RECEIVED

6 October 2021

REVISED

15 March 2022

ACCEPTED FOR PUBLICATION



21 March 2022

PUBLISHED

8 June 2022

Original content from this work may be used under the terms of the [Creative Commons Attribution 4.0 licence](#).

Any further distribution of this work must maintain attribution to the author(s) and the title of the work, journal citation and DOI.

Johannes Boy¹, Rüdiger Mitdank¹, Zbigniew Galazka²  and Saskia F Fischer^{1,*} ¹ Novel Materials Group, Humboldt-Universität zu Berlin, Newtonstraße 15, 12489 Berlin, Germany² Leibniz-Institut für Kristallzüchtung, Max-Born-Straße 2, 12489 Berlin, Germany

* Author to whom any correspondence should be addressed.

E-mail: boy@physik.hu-berlin.de and saskia.fischer@physik.hu-berlin.de**Keywords:** zinc gallate ZnGa₂O₄, thermal diffusivity, thermal conductivity, specific heat capacity, boundary scattering, umklapp scattering, phonon mean free path**Abstract**

This work provides the first experimental determination of the low-temperature thermal properties for novel highly pure single-crystalline ZnGa₂O₄. The temperature dependence of the thermal conductivity, diffusivity and specific heat capacity of as-grown, degenerated ZnGa₂O₄ single crystals is measured using the 2ω -method between $T = 27$ K and room temperature. At room temperature the thermal diffusivity is $D \approx 6.9 \cdot 10^{-6} \text{ m}^2\text{s}$, the thermal conductivity is $\lambda \approx 22.9 \text{ W mK}^{-1}$ and the specific heat capacity is $C_V \approx 537 \text{ J kgK}^{-1}$. The thermal conductivity increases with decreasing temperatures due to reduced phonon-phonon Umklapp scattering down to $T = 50$ K. For lower temperatures the thermal conductivity is limited by boundary scattering.

1. Introduction

Only recently, has the transparent semiconducting wide-bandgap oxide ZnGa₂O₄ been successfully grown as single crystals using the vertical gradient freeze method [1]. These novel ZnGa₂O₄ single crystals may find possible applications as a substrate material for homo- or heteroepitaxial growth in high-power electronics, gas sensors or optical devices [1–5]. Full transparency in the visible and near infrared spectral regions is given by the optical absorption edge at 275 nm. The optical bandgap extracted from the absorption coefficient is direct with a value of about 4.6 eV, close to that of β -Ga₂O₃. ZnGa₂O₄ is cubic ($Fd\bar{3}m$ space group) with a normal spinel structure in which Zn²⁺ and Ga³⁺ cations are distributed in tetrahedral and octahedral lattice sites, respectively [6]. Therefore, it may provide a good lattice-matched substrate for magnetic Fe-based spinel films and because ZnGa₂O₄ is a cubic system with no distinguished cleavage planes it may enable the growth of large volume crystals and wafer fabrication [1]. It was shown that the thermal conductivity of ZnGa₂O₄ is isotropic at room temperature with the value of about $22 \text{ W m}^{-1} \text{ K}^{-1}$ measured by a laser flash technique [1] and therefore similar to that of β -Ga₂O₃ along the [001] axis [7].

While the low-temperature electrical and thermo-electrical transport properties have recently been studied [2], the low-temperature thermal properties of single crystalline ZnGa₂O₄, such as the thermal conductivity, the thermal diffusivity and the specific heat capacity, remain unexplored. However, these thermal material parameters are important for the understanding of charge and heat scattering mechanisms in novel devices.

Here, we provide the first experimental determination of the temperature-dependent thermal conductivity, diffusivity and specific heat capacity of as-grown, degenerate single-crystalline ZnGa₂O₄. Therefore, the 2ω -method [7, 8] is implemented, which consists of microfabricated metal heater and sensor lines to induce and detect temperature oscillations by applying AC currents and measuring voltages. This method allows the simultaneous determination of thermal conductivity and diffusivity. Therefore, the Debye temperature and the mean free path can be determined as a function of temperature. We discuss the scattering mechanisms that dominate the phonon transport and apply the Debye-model to the specific heat capacity, which yields an approximation for the Debye-temperature.

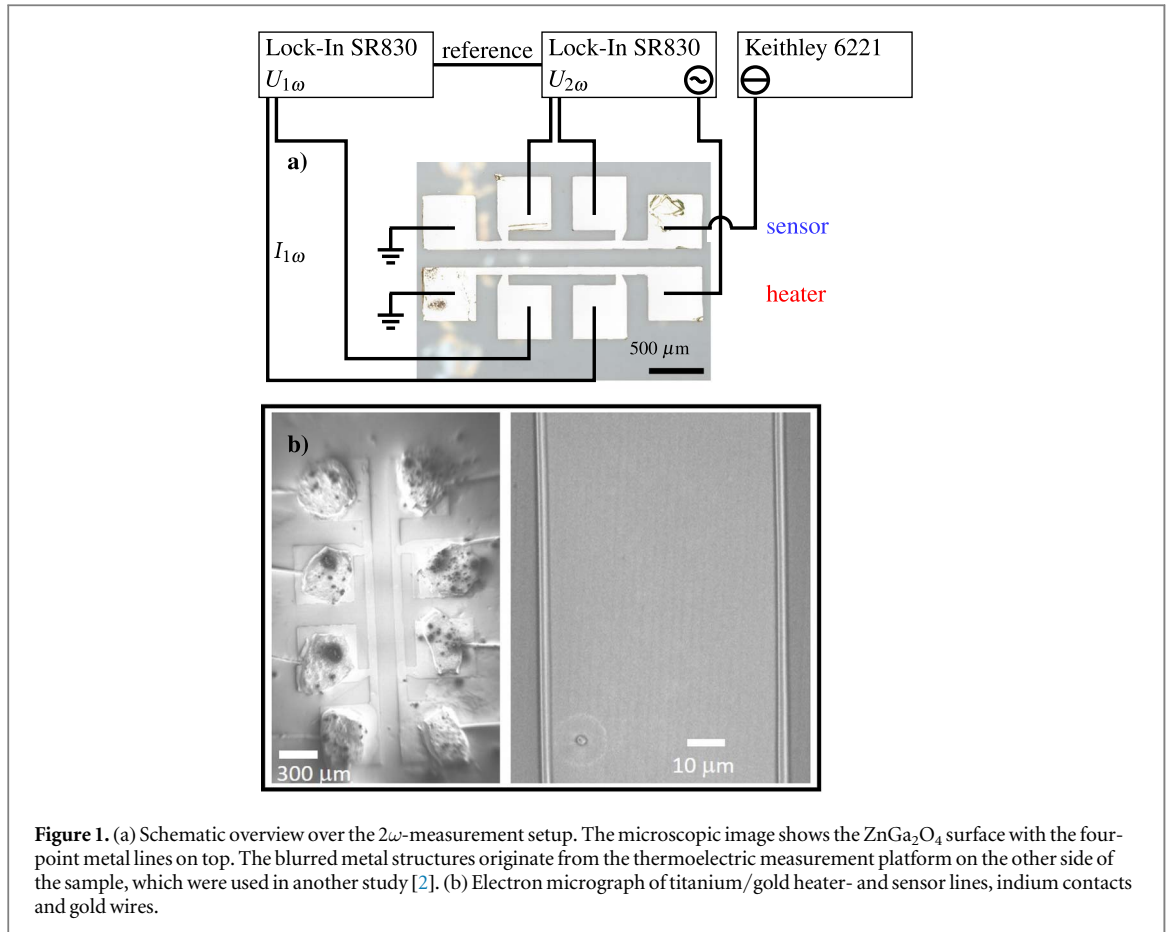


Figure 1. (a) Schematic overview over the 2ω -measurement setup. The microscopic image shows the ZnGa_2O_4 surface with the four-point metal lines on top. The blurred metal structures originate from the thermoelectric measurement platform on the other side of the sample, which were used in another study [2]. (b) Electron micrograph of titanium/gold heater- and sensor lines, indium contacts and gold wires.

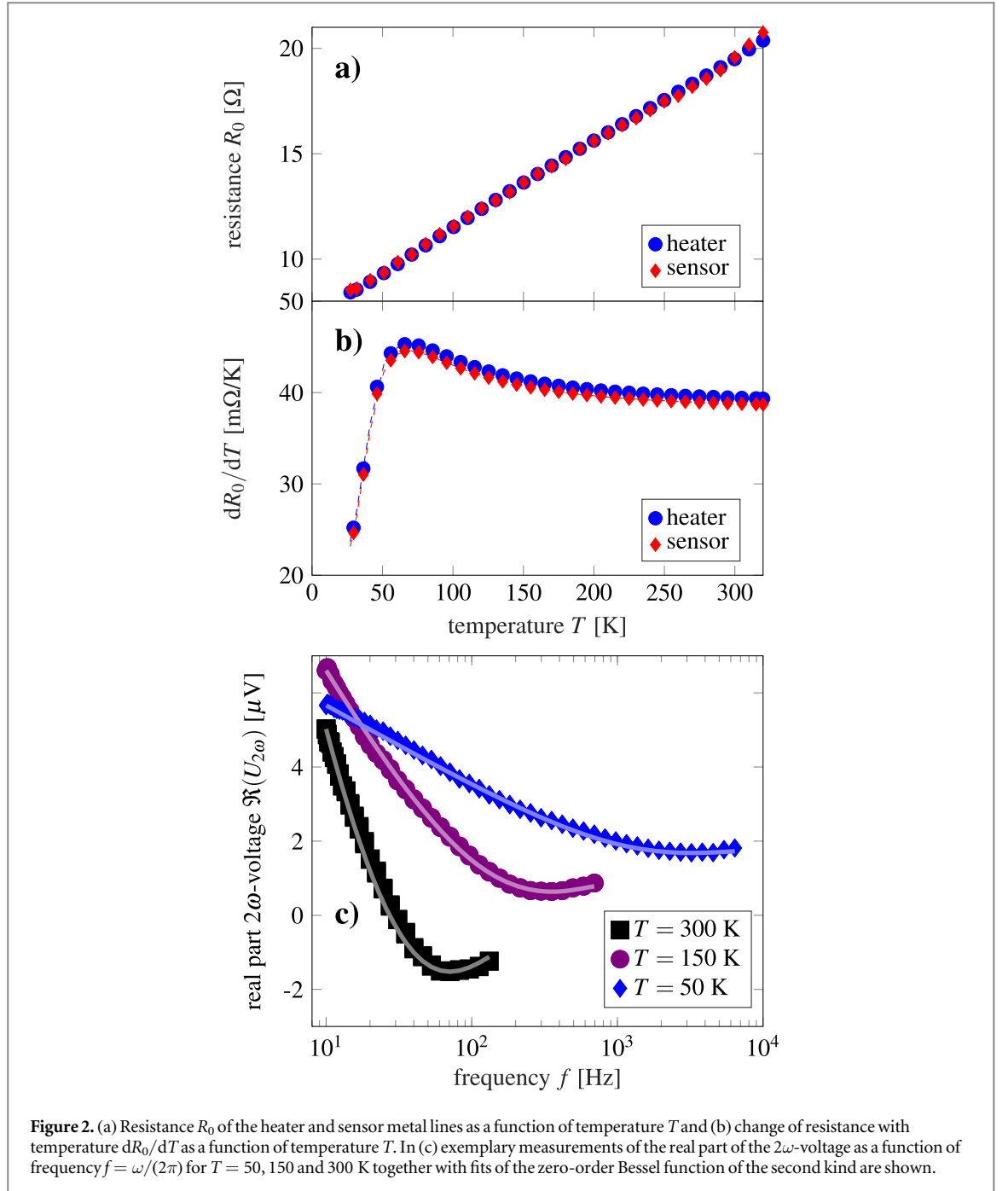
2. Materials and methods

The measurement setup used here consists of the electrically conducting ZnGa_2O_4 bulk sample and one pair of metallic heater lines on its surface. The metallic four-point lines serve as a heater and sensor and can be seen as a microscopic image in figure 1(a).

The sample was grown using the vertical gradient freeze method [1]. The starting materials were ZnO and Ga_2O_3 with a purity of 99.999% each and no intentional doping. The growth was performed in an O_2/Ar atmosphere and resulted in a transparent single crystal of bluish coloration. The resulting crystals have a composition close to stoichiometric, without cracks, twins, and low-angle grain boundaries. Transmission electron microscopy bright field images have revealed Moiré patterns that could originate from nano-particles of metallic nature and lattice distortion [1]. Further details are available in Galazka *et al* [1], in particular regarding the growth method and parameters, structural and chemical characterization including micrographs of the bulk crystal and cut-wafer pieces ([1]: figure 2), x-ray diffraction pattern ([1]: figures 8, 10) and high-resolution transmission electron microscopy image ([1]: figure 12) as well as the electric and thermoelectric properties [1, 2].

The four-point metal lines consist of titanium (7 nm) and gold (35 nm). They were patterned by standard photolithography, magnetron sputtering and lift-off processing after cleaning with acetone, isopropanol and subsequent drying in N_2 . The as-sputtered metal lines form a Schottky contact relative to the ZnGa_2O_4 , with a dynamic resistance greater than $R_{\text{dyn,sch}} \geq 1000 \Omega$ [2]. By electrical contacting with gold wire and indium, see figure 1(b), the metal lines stayed isolated from each other and the ZnGa_2O_4 . This method has proven successful before [2, 9, 10]. Electron micrographs were taken by a Raith Pioneer II system.

The 2ω -measurement setup [8] is shown in figure 1(a) and works as follows. The right Lock-In amplifier (SR 830) creates oscillating joule heating in the heater metal line. The heating power P is measured by the left Lock-In amplifier (SR 830). A constant current source unit (Keithley 6221) imprints a current into the sensor line. The temperature oscillations ΔT are measured as a 2ω -voltage oscillation $U_{2\omega}$ by the right Lock-In amplifier. The measurements are carried out in a pulse tube cryocooler under vacuum between 20 K and room temperature. The 2ω -method allows the determination of the thermal properties in any crystal orientation. However, since the spinel crystal structure forms a cubic lattice, no anisotropy of the thermal diffusivity and conductivity is expected.



The joule heating is created by an alternating current, leading to the temperature oscillation [11] $\Delta T \propto P = (U_0 I_0/2) \cdot (1 + \cos(2\omega t))$, with the voltage amplitude U_0 , current amplitude I_0 , angular frequency of the oscillation ω and time t . The temperature oscillations ΔT are detected by the change of the resistance of the sensor line $R = R_0 + dR_0/dT \cdot \Delta T$, with R_0 the resistance of the sensor line at the given bath temperature T . The temperature dependence of the sensor and heater metal lines is depicted in figure 2(a) and follows the Bloch-Grüneisen-relation [12]. The change of resistance with temperature dR_0/dT is obtained from numerical differentiation and shown in figure 2(b). The overall temperature oscillation in the sensor line ΔT_S is detected from the $U_{2\omega}$ signal

$$U_{2\omega} = \frac{(dR_{S,0}/dT) I_{S,DC} \sqrt{2}}{2} \Delta T_S, \quad (1)$$

with the change of the resistance of the sensor line with temperature $dR_{S,0}/dT$, sensor detection current $I_{S,DC}$.

The thermal properties are determined from the frequency dependence of the 2ω -voltage signal $U_{2\omega}$. The solution of the thermal conduction differential equation for an oscillating temperature is

$$\Delta T(r) = \frac{P}{\pi L_H \lambda} \cdot K_0(qr), \quad (2)$$

with the heater power per unit length of the heater P/L_H , the thermal conductivity of the ZnGa_2O_4 λ , the zero-order Bessel function of the second kind K_0 , the inverse thermal penetration depth $q = \sqrt{2\omega/D}$ and the thermal diffusivity D [13]. Figure 2(c) shows exemplary data of the real part of the 2ω -voltage $\Re(U_{2\omega})$ as a function of frequency for $T = 50, 150$ and 300 K. The solid lines represent the fits. The thermal diffusivity is obtained from the position of the minimum, and the thermal conductivity depends on the slope at low frequencies.

The geometry and width of the metal lines have to be considered as well [8]

$$\Delta T = \frac{P}{\pi L_H \lambda} \frac{1}{2w_H} \int_{-w_H}^{w_H} \frac{1}{2w_S} \cdot \int_{-w_S}^{w_S} K_0(q \cdot (d + o - p)) \, do \, dp. \quad (3)$$

Here w_H and w_S denote half the line width of the heater and sensor line, respectively. Here, ΔT_S is retrieved from equations (2) and (3) for the distance from heater to sensor line $r = 250 \mu\text{m}$. More details on the 2ω -method can be found in the literature [7, 8].

3. Results

The results for the thermal diffusivity D , thermal conductivity λ and specific heat capacity C_V as a function of (inverse) temperature can be seen in figure 3 and table 1. The thermal diffusivity D in figure 3(a) shows a power-law increase with decreasing temperature. This is attributed to phonon-phonon interaction limiting the thermal conductivity and will be evaluated subsequently for the phonon mean free path Λ . At temperatures below $T \leq 70$ K the dominant scattering process changes, leading to a change of temperature dependency.

In figure 3(b) the thermal conductivity λ is depicted. The room temperature value is $\lambda(T = 300\text{K}) \approx 22.9 \text{ W mK}^{-1}$ and agrees well with the previously reported value [1] $\lambda(T = 300\text{K}) \approx 22.1 \text{ W mK}^{-1}$ measured by a laser flash technique. The thermal conductivity also increases with decreasing temperature with $\lambda \propto T^{-1}$, forms a maximum of $\lambda \approx 154 \text{ W mK}^{-1}$ at around $T = 50$ K and decreases for lower temperatures. This temperature dependence was observed before [2] and could be due to a distortion of the lattice that was previously observed as Moiré patterns [1].

The thermal conductivity has an electronic and a phononic contribution $\lambda = \lambda_e + \lambda_{ph}$. The electronic part of the thermal conductivity can be estimated by the Wiedemann-Franz-relation [14]

$$\lambda_e = L_0 T \sigma, \quad (4)$$

with the Lorentz-constant L_0 and the electrical conductivity σ . For $T = 300$ K $\sigma \approx 287 \text{ S cm}^{-1}$ [2] leading to a negligible electronic contribution of $\lambda_e \approx 0.22 \text{ W mK}^{-1}$ that decreases with decreasing temperature. Hence the dominant heat transport in ZnGa_2O_4 is by phonons.

The specific heat capacity is calculated by

$$C_V = \frac{\lambda}{D \cdot \rho}, \quad (5)$$

with the mass density of ZnGa_2O_4 [15] $\rho = 6.2 \text{ g cm}^{-3}$, which is assumed constant for the investigated temperatures. Starting from low temperatures, the specific heat capacity increases due to an increase of occupied phonon modes. The non-saturated room temperature value is $C_V \approx 540 \text{ J kgK}^{-1}$. Additionally, four fits of the Debye-model [16] are shown

$$C_V = 9Nk_B \left(\frac{T}{\Theta_D} \right) \int_0^{\Theta_D/T} \frac{x^4 e^x}{(e^x - 1)^2} dx, \quad (6)$$

with the number of atoms N , Boltzmann constant k_B and Debye temperature Θ_D . The fits with Debye temperatures of $\Theta_D = 600$ and 700 K reproduce the data best. The deviation of the fit from the data at low temperatures is due to the complex crystal structure of ZnGa_2O_4 and the lattice distortion mentioned before.

4. Discussion

The temperature dependence of the phonon mean free path Λ gives insight into the dominant phonon scattering mechanisms and is shown in figure 4(a). It was calculated assuming a temperature independent sound velocity of ZnGa_2O_4 [15] of $v = 7849 \text{ m s}^{-1}$ using $\Lambda = 3D/v$. The room temperature value is $\Lambda(T = 300\text{K}) \approx 2.5 \text{ nm}$ that increases with decreasing temperature to $\Lambda(T = 27\text{K}) \approx 170 \text{ nm}$. For $T = 100$ to 300 K the data is well explained by phonon Umklapp scattering as shown in figure 4(a) by the dashed line. At lower temperatures the data is well explained by adding boundary scattering with a mean distance of the boundaries of $d_{\text{boundary}} \approx 170 \text{ nm}$, see the dash-dotted line and the combined fit as a solid line in figure 4(a). The boundary scattering may be caused by the

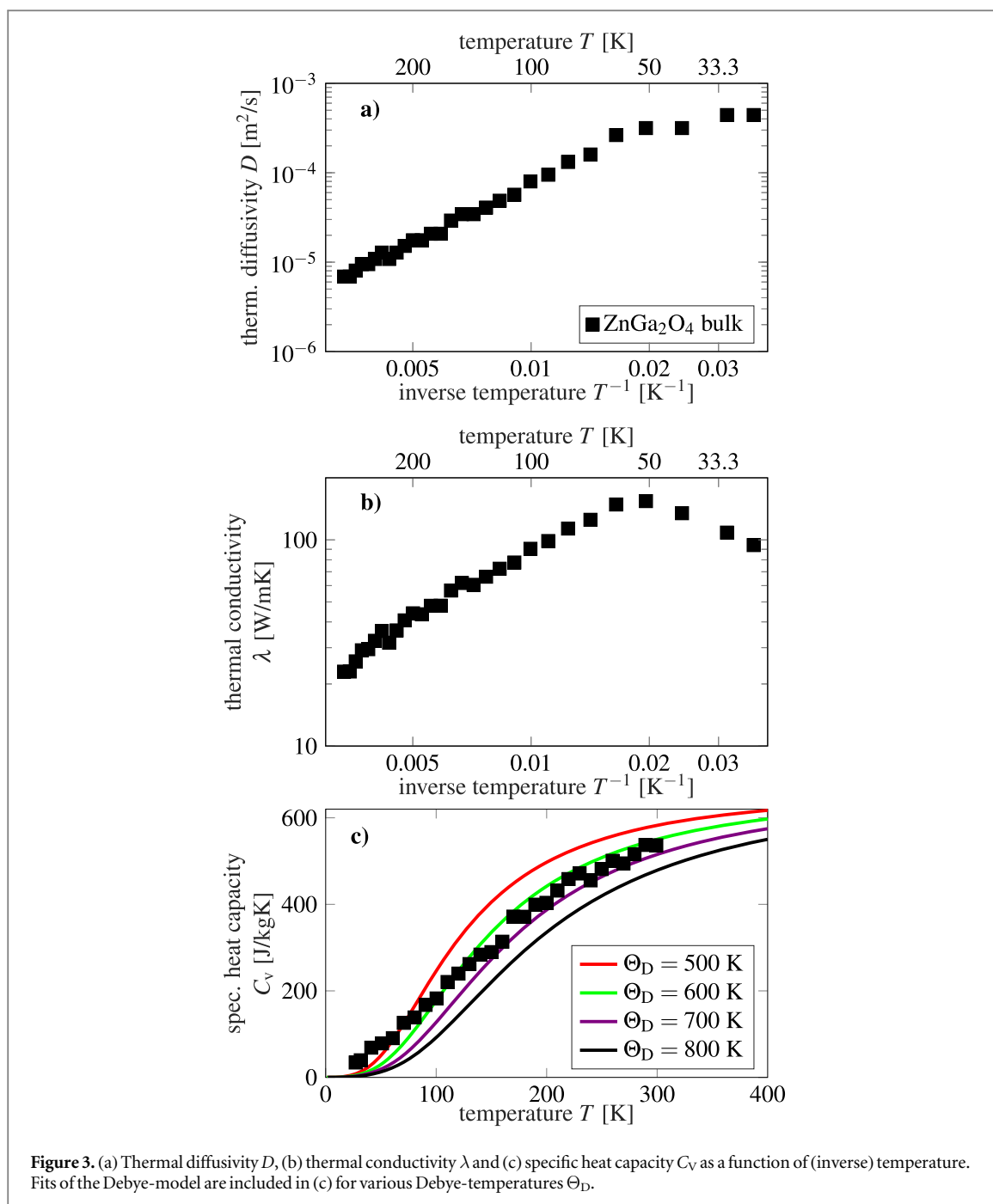
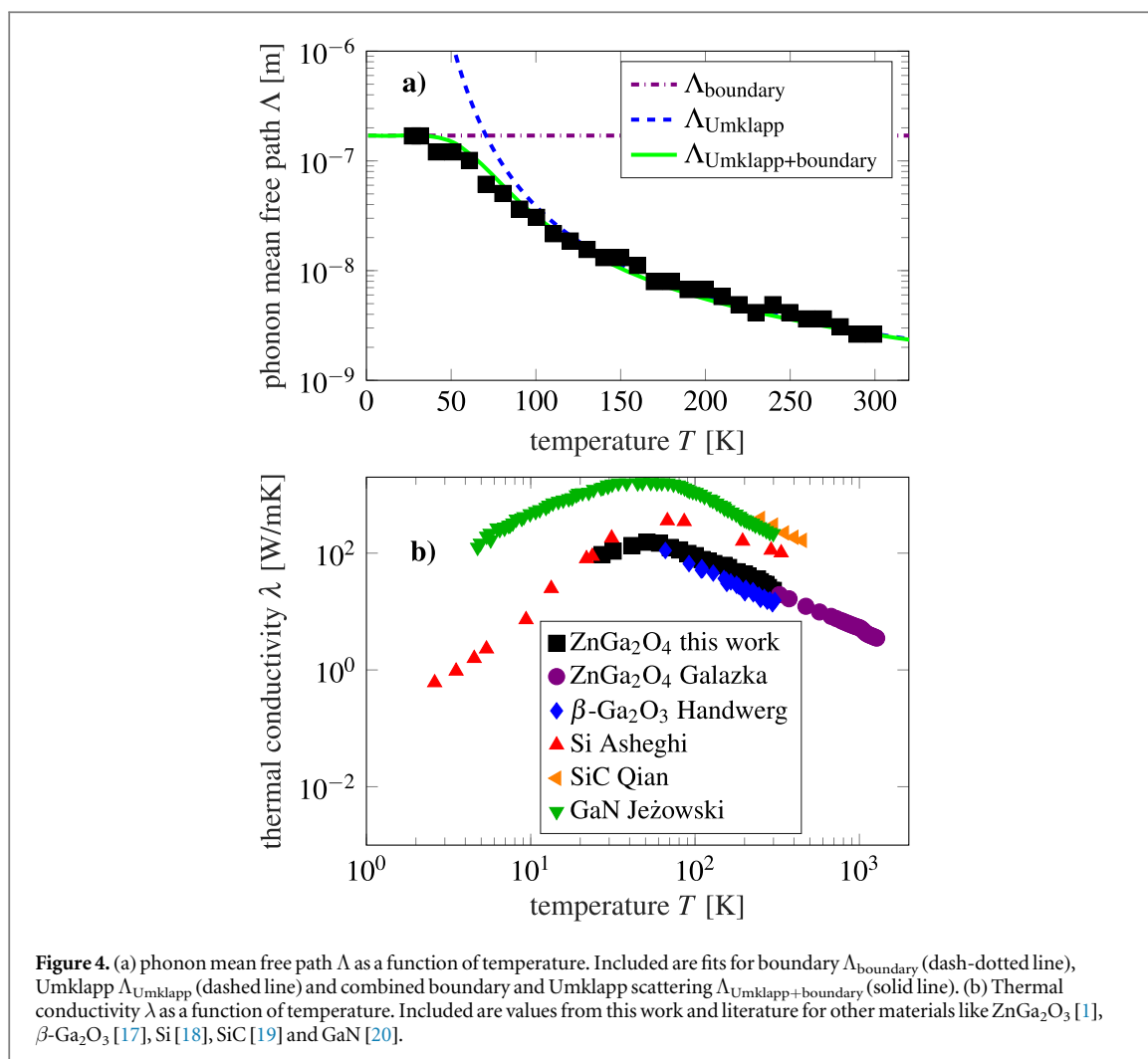


Table 1. Values for the thermal diffusivity D , thermal conductivity λ , specific heat capacity C_V and phonon mean free path Λ for $T = 27$ K, 50 K and 300 K.

T [K]	27	50	300
D [$10^{-6} \cdot \text{m}^2 \text{s}^{-1}$]	442	316	7
λ [W/mK]	94	154	22.9
C_V [J/kgK]	34	78	536
Λ [nm]	168	120	2.6

deformation of the lattice, which was observed as Moiré patterns in transmission electron microscopy bright field images and had an average distance of about 120 nm [1, 2].

The thermal conductivity of semiconductors is an important parameter for the heat management in electrical devices, in particular for wide-bandgap semiconductors in use for power electronics. The results from



this work are compared to values from the literature and other materials in figure 4(b). It can be seen that the results of this work using the 2ω -method fit well with the room temperature values of ZnGa₂O₄ from Galazka *et al* [1]. Furthermore, the thermal conductivity is well comparable to that of the sesquioxide β -Ga₂O₃ [7, 17], both being an order of magnitude lower than that of silicon [18] and silicon carbide [19]. However, the thermal conductivity of ZnGa₂O₄ may be increased at low temperatures, if the cause for boundary scattering, i.e. lattice defects, is reduced or eliminated.

5. Summary

In summary, we provide the first experimental determination of the low-temperature thermal properties of as-grown single-crystalline ZnGa₂O₄. The simultaneous determination of the thermal conductivity and diffusivity were enabled by the 2ω -method, for which metal lines with a Schottky barrier were fabricated to electrically conducting ZnGa₂O₄. At room temperature the thermal conductivity is $\lambda(T = 300\text{K}) \approx 22.9 \text{ W mK}^{-1}$ and for temperatures above 100 K the phonon transport is limited by phonon Umklapp scattering. At lower temperatures boundary scattering at lattice defects limits the thermal conductivity to $\lambda(T = 27\text{K}) \approx 95 \text{ W mK}^{-1}$. Thus, if the cause for boundary scattering, i.e. lattice defects, is reduced or eliminated, the thermal conductivity of ZnGa₂O₄ may be increased at low temperatures.

Acknowledgments

The authors thank Dr. Martin Handweg for scientific and technical support and Dr. Detlef Klimm from the Leibniz-Institut für Kristallzüchtung for critical reading of the manuscript. This work was performed in the framework of GraFOx, a Leibniz-ScienceCampus partially funded by the Leibniz Association and by the German Science Foundation (DFG-FI932/10-1, DFG-FI932/10-2).

Data availability statement

All data that support the findings of this study are included within the article (and any supplementary files).

Competing interests

The authors declare no competing interests.

ORCID iDs

Zbigniew Galazka  <https://orcid.org/0000-0003-0812-2873>

Saskia F Fischer  <https://orcid.org/0000-0002-1088-3615>

References

- [1] Galazka Z *et al* 2019 Ultra-wide bandgap, conductive, high mobility, and high quality melt-grown bulk $ZnGa_2O_4$ single crystals *PL Materials* **7** 022512
- [2] Boy J, Handweg M, Mitdank R, Galazka Z and Fischer S F 2020 Charge carrier density, mobility, and seebeck coefficient of melt-grown bulk $ZnGa_2O_4$ single crystals *IP Advances* **10** 055005
- [3] Grundmann M, Frenzel H, Lajn A, Lorenz M, Schein F and von Wenckstern H 2010 Transparent semiconducting oxides: materials and devices *Physica Status Solidi (a)* **207** 1437–49
- [4] Lorenz M *et al* 2016 The 2016 oxide electronic materials and oxide interfaces roadmap *J. Phys. D: Appl. Phys.* **49** 433001
- [5] Fortunato E, Barquinha P and Martins R 2012 Oxide semiconductor thin-film transistors: A review of recent advances *Adv. Mater.* **24** 2945–86
- [6] Brik M G, Suchocki A and Kamińska A 2014 Lattice parameters and stability of the spinel compounds in relation to the ionic radii and electronegativities and constituting chemical elements *Inorg. Chem.* **53** 5088–99
- [7] Handweg M, Mitdank R, Galazka Z and Fischer S F 2016 Temperature-dependent thermal conductivity and diffusivity of a Mg-doped insulating β - Ga_2O_3 single crystal along [100], [010] and [001] *Semicond. Sci. Technol.* **31** 125006
- [8] Ramu A T and J E Bowers 2012 A ‘2-omega’ technique for measuring anisotropy of thermal conductivity *Rev. Sci. Instrum.* **83** 124903
- [9] Boy J, Handweg M, Ahrling R, Mitdank R, Wagner G, Galazka Z and Fischer S F 2019 Temperature dependence of the seebeck coefficient of epitaxial β - Ga_2O_3 thin films *APL Mater.* **7** 022526
- [10] Ahrling R, Boy J, Handweg M, Chiatti O, Mitdank R, Wagner G, Galazka Z and Fischer S F 2019 Transport properties and finite size effects in β - Ga_2O_3 thin films *Sci. Rep.* **9** 13149
- [11] Cahill D G 1990 Thermal conductivity measurement from 30 to 750 K: the 3ω method *Rev. Sci. Instrum.* **61** 802–8
- [12] Tritt T M 2010 *Thermal Conductivity: Theory, Properties, and Applications* (US: Springer)
- [13] Cahill D G and Pohl R O 1987 Thermal conductivity of amorphous solids above the plateau *Phys. Rev. B* **35** 4067–73
- [14] Franz R and Wiedemann G 1853 Über die wärme-leitungsfähigkeit der metalle *Annalen der Physik und Chemie* **165** 497–531
- [15] Zerarga F, Bouhemadou A, Khenata R and Binomran S 2011 FP-LAPW study of the structural, elastic and thermodynamic properties of spinel oxides ZnX_2O_4 (X = Al, Ga, In) *Comput. Mater. Sci.* **50** 2651–7
- [16] Hunklinger S 2009 *Festkörperphysik vol 2* (München: Oldenbourg Verlag)
- [17] Handweg M, Mitdank R, Galazka Z and Fischer S F 2015 Temperature-dependent thermal conductivity in Mg-doped and undoped β - Ga_2O_3 bulk crystals *Semicond. Sci. Technol.* **30** 024006
- [18] Ashghi M, Kurabayashi K, Kasnavi R and Goodson K E 2002 Thermal conduction in doped single-crystal silicon films *J. Appl. Phys.* **91** 5079–88
- [19] Qian X, Jiang P and Yang R 2017 Anisotropic thermal conductivity of 4H and 6H silicon carbide measured using time-domain thermoreflectance *Materials Today Physics* **3** 70–5
- [20] Jezowski A, Bockowski B A, Grzegory I, Krukowski S, Suski T and Paszkiewicz T 2003 Thermal conductivity of GaN crystals in 4.2–300 K range *Solid State Commun.* **128** 69–73